Journal of Applied Physics

# Magnetic resonance in $Fe_xMn_{1-x}S$ single crystals

Cite as: J. Appl. Phys. **106**, 073909 (2009); https://doi.org/10.1063/1.3234402
Submitted: 29 June 2009 . Accepted: 25 August 2009 . Published Online: 09 October 2009

**A. M. Vorotynov, G. M. Abramova, M. A. Popov, G. A. Petrakovskii, A. F. Bovina, V. V. Sokolov, and E. Mita**









AIP Publishing

# Magnetic resonance in $Fe_xMn_{1-x}S$ single crystals

A. M. Vorotynov,[1,a)] G. M. Abramova,[1] M. A. Popov,[1] G. A. Petrakovskii,[1] A. F. Bovina,[1] V. V. Sokolov,[2] and E. Mita[3]
[1]*Kirensky Institute of Physics, Russian Academy of Sciences, Siberian Branch, Krasnoyarsk, 660036 Russia*
[2]*Nikolaev Institute of Inorganic Chemistry, Russian Academy of Sciences, Siberian Branch, Novosibirsk, 630090 Russia*
[3]*Osaka University, Toyonaka, 560-8531 Japan*

(Received 29 June 2009; accepted 25 August 2009; published online 9 October 2009)

The results of the experimental study and computer simulation of the resonance spectra of a single crystal of the iron-manganese sulfide $Fe_xMn_{1-x}S$ $(0 \leq x \leq 0.29)$ are presented. The resonance properties of the concentrated solid solutions are explained by the formation of a homogeneous $Fe_xMn_{1-x}S$ matrix with randomly distributed superparamagnetic iron nanoparticles. The mean diameter ($\langle D \rangle = 6.19$ nm at $T=250$ K) and the axial first-order anisotropy constant ($K_1 = 4.08$ erg/cm$^3$ at $T=250$ K) of the ferromagnetic particles are determined. The volume fraction of the iron phase is estimated. © *2009 American Institute of Physics*. [doi:10.1063/1.3234402]

## I. INTRODUCTION

Solid solutions of manganese oxides and sulfides have been studied intensively since the discovery of the metal-dielectric transitions and colossal magnetoresistance in these materials. At present, oxide compounds of the manganite class are the best studied. The available experimental data on the sulfide solid solutions are insufficient and often contradictory in virtue of a complexity of the synthesis of these materials.[1]

The manganese monosulfide MnS possessing of a face-centered cubic (fcc) lattice of the NaCl type (*Fm*-3*m* space group) is a classic antiferromagnet with the strong electron correlations,[1,2] similar to $LaMnO_3$. It was shown[3–5] that in the $Fe_xMn_{1-x}S$ $(0 \leq x \leq 0.29)$ system with an increase in cation substitution degree, a concentration electron transition occurs, which is accompanied by five orders of magnitude drop of the resistivity in the paramagnetic state.

It was established[3] that in the $Fe_xMn_{1-x}S$ samples with an increase in iron concentration, the Neel temperature increases from $T_N = 147$ K at $x=0$ to $T_N = 190$ K at $x=0.29$. Surprisingly, above the temperature of the magnetic phase transition, the hysteresis loops were observed.[3] We suggest that this fact is related to the structural inhomogeneity, i.e., the presence of secondary phase that appears during synthesis. When the volume of the secondary phase is sufficiently small, it is fairly difficult to reveal its presence by the x-ray methods or Mössbauer spectroscopy. The method sensitive to the presence of magnetic phases in a sample is the magnetic resonance. In our case, the problem is simplified by the fact that the paramagnetic phase of the $Fe_xMn_{1-x}S$ matrix should be separated from the secondary magnetically ordered phase, which yields the hysteresis loop at high temperatures.

In order to investigate the magnetic properties of the iron-manganese sulfides, the $Fe_xMn_{1-x}S$ $(0 \leq x \leq 0.29)$ single crystals were synthesized and studied by the magnetic resonance method in the temperature range of 90–300 K.

a)Electronic mail: sasa@iph.krasn.ru.

## II. SAMPLES AND EXPERIMENTAL TECNIQUE

The synthesis of the $Fe_xMn_{1-x}S$ single crystals is described in detail in Refs. 3 and 4. First, the polycrystalline samples were grown from the stoichiometric mixture of the oxides and iron by the sulfidizing method. From the obtained powder, the single crystals were grown by the spontaneous crystallization method. The synthesized single crystals were cylinders with a diameter and length of about 1 cm. For the resonance measurements, the smaller samples were prepared by splitting the single crystals along their cleavage planes. The $Fe_xMn_{1-x}S$ samples with an iron concentration $0 \leq x \leq 0.29$ as that in the charge were studied. The results of the x-ray diffraction analysis performed with a DRON diffractometer (Cu $K_\alpha$–irradiation) were reported in Refs. 4 and 5. The x-ray fluorescence study was carried out with an Element Analyzer JSX-3600 JEOL (Japan). The resonance properties were investigated with an *X*-band SE/X-2544 spectrometer in the temperature range of 90–300 K.

## III. EXPERIMENTAL RESULTS AND DISCUSSION

The x-ray phase analysis showed[4,5] with 5% accuracy that the $Fe_xMn_{1-x}S$ samples with $0 \leq x \leq 0.29$ are single-phase solid solutions with the cubic NaCl crystal structure typical of the $\alpha$-manganese monosulfide. Upon cation substitution of iron ions for manganese ions, the cubic NaCl lattice is compressed similar to the MnS compound at room temperature under pressure. At room temperature, the parameters of the fcc lattice of the $Fe_xMn_{1-x}S$ samples change from $a = 5.22$ Å at $x=0$ to 5.166 Å at $x=0.29$. The x-ray fluorescence analysis shows that iron concentration $x$ in the charge differs from iron concentration $x_S$ in the real solid solution. In particular, for the single crystals with $x=0.05$ and 0.10, the iron concentration values in the real solid solutions are $x_S = 0.06 \pm 0.02$ and $0.119 \pm 0.007$, respectively. In some cases, in the single crystals with higher iron concentration the coexistence of the solid solutions with different component ratios is observed. In particular, for the single crystal with $x=0.15$, the average concentration value corresponds to

 

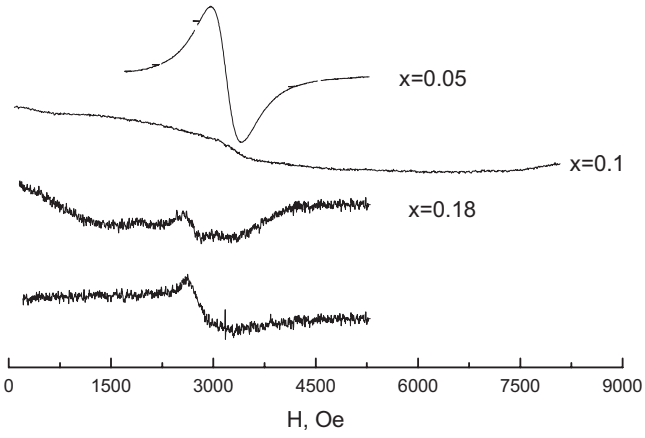


FIG. 1. Evolution of the resonance spectra of the $Fe_xMn_{1-x}S$ compounds for different $x$ at room temperature.

$x_S=0.12\pm0.04$. However, two sides of the same single-crystal sample correspond to the two different iron concentration values $x_S=0.097\pm0.006$ and $0.14\pm0.02$. Thus, one can conclude that the single crystals of the $Fe_xMn_{1-x}S$ solid solutions with higher iron concentration are characterized by the inhomogeneous distribution of iron ions over the single crystal volume. Hereinafter, iron concentration $x$ is given according to the charge composition of the samples under study.

Figure 1 depicts the change in the magnetic resonance spectrum as a function of iron concentration. At room temperature, the *X*-band magnetic resonance spectrum of the sample with $x=0.05$ represents a symmetric Lorentz line with the linewidth $\Delta H=470$ Oe and a $g$ factor of 1.999. The obtained spectrum and its temperature and angle dependence are identical to those of the MnS compound studied previously.[6] The magnetic resonance spectrum significantly changes with an increase in iron concentration. In particular, at $x=0.1$ the spectrum is a broad absorption line with the linewidth $\Delta H=6000$ Oe, $g=1.999$, and the intensity lower than that of the sample with the $x=0.05$ by an order of magnitude. Such a significant difference between the spectra can be attributed to both the enhancement in the covalence contribution to the chemical bond, which is pointed by the change in the isomeric shift,[4,5] and the growth of metallization of the samples. The electrical resistance of $Mn_{1-x}Fe_xS$ changes from $\sim10^5$ Ω cm at $x=0$ to $\sim10^{-1}-10^{-2}$ Ω cm at $x=0.18$ and 0.29. With a further increase in iron concentration ($x=0.18$ and 0.29) the magnetic resonance spectrum transforms to the low intensity isotropic (without angular dependence) compound signal with the narrow line superposed with a broader one. The signal typical of $Mn^{2+}$ ions is completely absent. As was mentioned above, for the samples with high iron concentration ($x>0.18$) at room temperature the hysteresis loops are observed, whereas the Neel temperature changes from 161 K ($x=0.05$) to 190 K ($x=0.29$). This may be caused by the occurrence of small amount of a secondary ferromagnetic phase, apparently iron containing, with the high temperature of magnetic ordering that cannot be found by the x-ray methods or Mössbauer spectroscopy.

The observed resonance spectra for the samples with $x\geq0.18$ do not drastically change at temperatures above and below the Neel temperature (Fig. 2). This fact allows assuming that the observed resonance signal does not belong to the host $Mn_{1-x}Fe_xS$ matrix. The literature review showed that the observed spectra ($x\geq0.18$) are very similar to the magnetic resonance spectrum of a superparamagnetic assembly of ferromagnetic crystalline single-domain particles.[7–10] In order to gain some insight into the possible nature of the magnetic particles, we performed computer simulation of the magnetic resonance signals of the reference compound. As was shown previously,[7–10] the magnetic resonance spectrum of an assembly of such particles can be calculated as

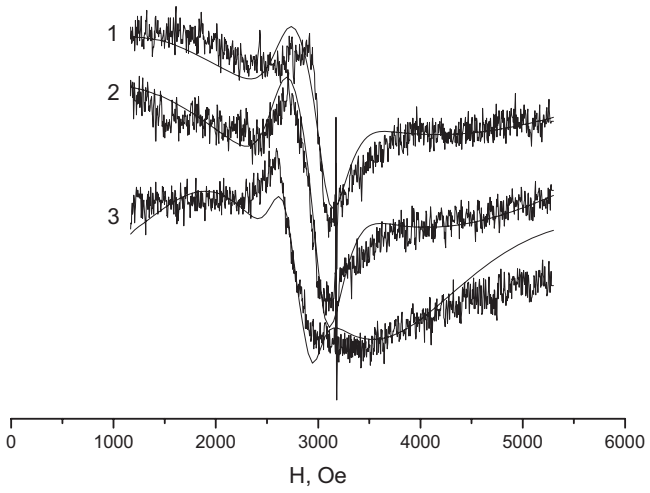


FIG. 2. Experimental and best-fit theoretical spectra for the $Fe_{0.29}Mn_{0.71}S$ sample at different temperatures. $1-T=92$ K, $2-T=120$ K, and $3-T=250$ K.

$$I(H)=\int_{\vartheta}\int_{\theta}\int_{D}F[H-H_{\text{eff}}(D,\vartheta,\theta),\Delta H]f_V(D)\sin\theta dDd\vartheta d\theta, \quad (1)$$

where $F[H-H_{\text{eff}}(D,\upsilon,\varphi),\Delta H]$ is the line shape function (Lorentzian or Gaussian), $\Delta H$ is the individual linewidth of a particle with a specified size, $H_{\text{eff}}$ is the resonance magnetic field which includes the external magnetic field, magnetic anisotropy field, and demagnetizing field, $D$ is the diameter of a particle, $\upsilon$ and $\varphi$ are the polar and azimuth angles between the external magnetic field, magnetic anisotropy field, and demagnetizing field, and $f_V(D)$ is the probability density of the volume fraction of the particles with diameter $D$. A number of the interrelated expressions for probability density $f_V(D)$ can be used. As a rule, the function is logarithmically normal[7]

$$f_V(D)=\frac{\exp(-\sigma^2/2)}{\sqrt{2\pi}\sigma D_{Vm}}\exp\left[-\frac{1}{2\sigma^2}\ln^2\frac{D}{D_{Vm}}\right], \quad (2)$$

where $D_{Vm}$ corresponds to the $f_V(D)$ maximum and $\sigma$ is the standard deviation of ln $D$. Quantities $D_{Vm}$ and $D_m$ (the most probable particle diameter) are interrelated as

$$D_{Vm}=D_m\exp(3\sigma^2). \quad (3)$$

The average diameter of a particle is[7]

TABLE I. The best-fit parameters obtained during the computer simulations of the $x=0.29$ sample magnetic resonance spectra at different temperatures. $D_m$ – the most probable particle diameter, $\langle D\rangle$—the mean particle diameter, $\sigma$—the standard deviation of ln $D$, $M_S$—the particle magnetization, $\Delta H$—the individual linewidth of the particle, and $K_1$—the axial first-order anisotropy constant.

| $T$ (K) | $D_m$ (nm) | $\langle D\rangle$ (nm) | $\sigma$ | $M_S$ (Oe) | $\Delta H$ (Oe) | $K_1$ ($10^5$ erg/cm$^3$) |
|---|---|---|---|---|---|---|
| 92 | 2.61 | 4.32 | 0.58 | 1755 | 2368 | 6.23 |
| 120 | 2.96 | 4.86 | 0.57 | 1655 | 2248 | 5.92 |
| 250 | 4.15 | 6.19 | 0.52 | 1721 | 1095 | 4.08 |

$$\langle D\rangle = D_m \exp\left(\frac{3}{2}\sigma^2\right). \quad (4)$$

We limit the discussion to the simplest case of the axial magnetic anisotropy[7] $[H_A=(K_1/M_S)(3\cos^2\theta-1)]$, a spherical shape of the particles, and the Gaussian line shape function. Then, during the computer simulation of the experimental spectra using Eq. (1), the fitting parameters are the following: $K_1$ is the first-order axial anisotropy constant, $M_S$ and $D$ are the particle magnetization and diameter, respectively, $\sigma$ is the standard deviation of the diameter of a particle from the most probable one, and $\Delta H$ is the individual resonance line width of a particle.

The results of fitting the experimental spectra to the theoretical curve obtained using Eq. (1) for the sample with $x=0.29$ at different temperatures are shown in Fig. 2. Table I presents the best-fit parameters.

First of all, it must be noted that, despite the simplified theoretical model was used, the values of best-fit parameters $M_S$ and $K_1$ obtained at the computer simulation are consistent with the corresponding values for pure iron. As is known,[11] crystalline iron has the saturation magnetization $M_s=1722$ Oe nearly constant up to the room temperature and the anisotropy constant values $K_1\approx 5.5\cdot 10^5$ erg/cm$^3$ at $T=100$ K and $4.9\times 10^5$ erg/cm$^3$ at $T=200$ K. The results obtained imply also that the interaction of the superparamagnetic iron particles with the host $Mn_{1-x}Fe_xS$ matrix is significantly weaker than the interactions of iron ions inside the particle.

The unanswered question is where the hysteresis loops originate from. As is known, the presence of the superparamagnetic particles does not cause the hysteresis phenomena during switching magnetization. Therefore, one may assume that in the host $Mn_{1-x}Fe_xS$ matrix, the iron particles large enough to stay nonparamagnetic are present. The magnetic parameters of these particles cannot be determined using the method described above because they do not contribute to the resonance signal.

Nevertheless, knowing the residual magnetization value at the temperatures $T>T_N$ ($M\approx 0.022$ emu and nearly temperature independent) and $M_S$ value, one can easily estimate the amount of the nonparamagnetic iron phase in the sample under study. It appeared less than 1%. Obviously, the concentration of this phase in the samples with $x<0.29$ is even less. Since the presence of the secondary phase was not confirmed by the other methods, we conclude that the total amount of the superparamagnetic and nonparamagnetic iron particles does not exceed 5%.

The values $\langle D\rangle$ and $\sigma$ obtained using the computer simulation (Table I) indicate the increase in average diameter and a decrease in its standard deviation with an increase in temperature. Note that these two trends compensate each other to a certain extent, so the volume fraction of the superparamagnetic particles in the sample weakly changes with temperature (Fig. 3). The same behavior was observed in Refs. 7 and 10.

In order to take into consideration the dependence of the linewidth on measurement temperature, the mechanisms of line broadening should be thoroughly analyzed. Usually, the spin-lattice interaction causes line broadening when the temperature increases. In our case, the opposite tendency is observed. A decrease in the linewidth with an increase in temperature can be attributed to "dynamic" modulation of "static" broadening. As a rule, inside a single-domain superparamagnetic nanoparticle the exchange interaction dominates. Also, one should take into account several other interactions; they are (1) the Zeeman interaction which tends to align the magnetic moments of the particles along the external magnetic field, (2) the magnetocrystalline anisotropy, which tends to align the magnetic moments along one of the easy magnetization axes and maintains the energy barriers between the directions, and (3) the thermal excitations which result in the fluctuations of orientation of the magnetic moments. In this context, the observed temperature dependence of linewidth $\Delta H$ can be attributed to the modulation of the magnetocrystalline anisotropy constant by the thermal fluc-

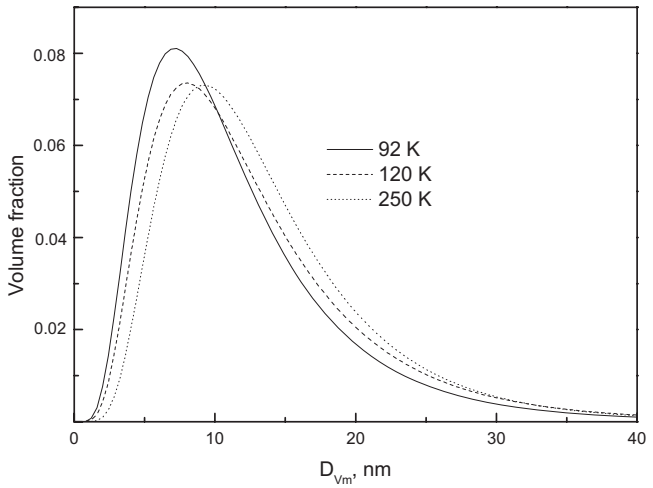


FIG. 3. Normalized volume fraction of nanoparticles vs their diameters for different temperatures obtained using the computer simulation of the magnetic resonance spectra (Table I).

tuations. An increase in temperature lowers anisotropy barriers and leads to the growth of the thermal fluctuations of the magnetic moments of the particles and the reduction in the linewidth.

## IV. CONCLUSIONS

The $Fe_xMn_{1-x}S$ ($0 \leq x \leq 0.29$) single crystals have been grown. The resonance properties of these compounds have been studied in the temperature range of 90–300 K. On the basis of the model proposed in Ref. 7, the resonance spectra for the sample with $x=0.29$ at different temperatures have been simulated. It has been shown that the features of the obtained spectra can be related to the presence of the small amount of the second ferromagnetic phase formed by the iron nanoparticles. The average diameter of the superparamagnetic nanoparticles has been determined and its temperature dependence has been established. The volume fraction of the secondary phase has been estimated.

## ACKNOWLEDGMENTS

This study was supported by the SB RAS–INTAS (Grant No. 06-1000013-9002) and the JSPS KAKENHI (Grant No. 18540317).

[1] G. V. Loseva, S. G. Ovchinnikov, and G. A. Petrakovskii, *Metal-Dielectric Transition in 3D Metal Sulfides* (Nayka, Novosibirsk, 1983), p. 144.
[2] G. M. Abramova and G. A. Petrakovskii, Fiz. Nizk. Temp. **32**, 954 (2006).
[3] G. Abramova, N. Volkov, G. Petrakovskiy, V. Sokolov, M. Boehm, O. Bajukov, A. Vorotynov, A. Bovina, and A. Pischjugin, J. Magn. Magn. Mater. **320**, 3261 (2008).
[4] G. Abramova, G. A. Petrakovskii, O. A. Bajukov, V. A. Varnek, V. V. Sokolov, and A. F. Bovina, Fiz. Tverd. Tela (St. Petersburg) **50**, 2 (2008).
[5] G. Abramova, G. A. Petrakovskii, O. A. Bajukov, A. F. Bovina, and V. V. Sokolov, Fiz. Tverd. Tela (Leningrad) (Sov. Phys. Solid State) (in press).
[6] A. M. Vorotynov and G. V. Loseva, Fiz. Tverd. Tela (Leningrad) **38**, 933 (1996).
[7] R. Berger, J. Kliava, J.-C. Bissey, and V. Baietto, J. Phys.: Condens. Matter **10**, 8559 (1998).
[8] R. Blinc, P. Cevc, A. Zorko, J. Holc, M. Kosec, Z. Trontelj, J. Pirnat, N. Dalal, V. Ramachandran, and J. Krzystek, J. Appl. Phys. **101**, 033901 (2007).
[9] R. S. de Biasi and T. C. Devezas, J. Appl. Phys. **49**, 2466 (1978).
[10] R. Berger, J. Kliava, J.-C. Bissey, and V. Baietto, J. Appl. Phys. **87**, 107389 (2000).
[11] *Tables of the Physical Values*, edited by I. K. Kikoin (Atomizdat, Moscow, 1976), p. 1006.